

# A tunable multiple-scattering system

John A. Scales and Kasper Van Wijk

*Center for Wave Phenomena, Department of Geophysics, Colorado School of Mines, Golden, CO 80401, USA*

## ABSTRACT

In order to study the propagation of multiply-scattered waves, it is useful to have a medium in which the scattering properties can be easily controlled. Here we describe such a system; it involves the propagation of ultrasonic surface waves in a medium with an aligned, disordered, pattern of small grooves. Waves propagating parallel to the grooves see a homogeneous medium; waves propagating perpendicular to the grooves are strongly scattered. By varying the source-receiver orientation with respect to the grooves and the distance between source and receiver, we are able to map out a smooth transition from ballistic to diffusive propagation. In addition, by using an optical detection system we are able to measure the wave motion *inside* the scattering medium. We measure the angle-dependent macroscopic properties of the medium, such as the phase and group velocity; but also the mean free path and the diffusion constant.

**Key words:** multiple scattering, Raleigh waves, diffusion

## 1 INTRODUCTION

The past 10 years have seen a tremendous growth of the interest within the physics community in understanding and exploiting multiply scattered waves. Recent work in medical imaging (Boas *et al.*, 1995) ultrasonics (Derode *et al.*, 1995) and seismology (Snieder, 1999), for example, has shown that multiply-scattered waves exhibit extraordinary stability (Scales & Snieder, 1999), in spite of the complexity of the wave fields, and can be exploited in a variety of ways to provide information about the scattering medium.

The influence of multiple scattering in wave propagation measurements can be seen in many ways. For example, there are subtle, long-wavelength effects such as anisotropy (if the scatterers are aligned) and attenuation (as energy is shifted from the ballistic pulse into the multiple-scattering coda) (Groenenboom & Snieder, 1995). These effects are well known in seismology (e.g., (Backus, 1962), (Aki & Chouet, 1975), (O'Doherty & Anstey, 1971)) and have been used to interpret effective material properties from macroscopic measurements. However, in most cases the same wave propagation phenomenon can be looked at from different points of view (such as ballistic propagation, diffusion or radiative transfer) depending, for example, on the wavelength

of the probing beam relative to the size of the disorder and on the distance propagated.

To understand these different regimes, describing the propagation of energy and their transitions, it would be extremely useful to have a medium in which the scattering properties could be easily adjusted. For example, with phonon scattering one can control the mean free path via the temperature (Wolfe, 1998). If the mean free path is greater or equal to the size of the sample, then the phonon propagates ballistically. The more scattering between source and receiver, the more diffusive the propagation. In (Bizheva *et al.*, 1998) the authors use path-length resolution to separate light propagating in a highly scattering system into components based on the degree of scattering.

In this paper we describe a simple laboratory model that we have used to study multiple scattering of ultrasonic surface waves. We are able to parametrically vary the strength of the scattering so that we can continuously and reproducibly change the material properties from no scattering to strong multiple-scattering. The model consists of a block of aluminum with 144 grooves in the pattern of a Fibonacci sequence etched into one face using a computer-controlled milling machine (Figure 1). An angle-beam transducer launches plane surface waves into this disordered medium and a laser-Doppler vibrometer measures the vertical component of particle

velocity on the surface. This setup allows us to measure multiply-scattered waves *inside* the scattering medium. The grooves are 1 mm wide by 3 mm deep and the dominant wavelength of the surface waves is about 15 mm, so there are many scatterers per wavelength when the waves are propagating perpendicular to the grooves. (See (Scales & Van Wijk, 1999), hereafter SVW, for more details on the model.)

In SVW we showed measurements of propagation parallel and perpendicular to the grooves. The result was that for propagation parallel to the grooves the surface wave propagated attenuation- and dispersion-free, whereas for propagation perpendicular to the grooves there was strong multiple scattering, causing long wavelength anisotropy and apparent attenuation. Here we extend these results to include the complete angle-dependent behavior of the scattering. We use the angle of propagation as a parameter to tune the scattering properties of the medium. We measured the angle-dependent group and phase velocities. We also describe how the multiple-scattering coda can be used to estimate both microscopic scattering properties such as the mean free path, and macroscopic material parameters such as the effective diffusion constant and attenuation.

## 2 EXPERIMENTAL SETUP AND MEASUREMENTS

The experimental setup is shown in Figure 1. A 200 V repetitive pulse is used to excite an angle-beam transducer mounted on the surface of an aluminum block of dimensions 28 cm  $\times$  23 cm  $\times$  21.5 cm. The transducer wedge has a footprint of 7 cm (in the forward direction) by 4.2 cm. To record the wave forms we used a laser-Doppler vibrometer (Polytec sensor head and vibrometer controller with a high-frequency decoder). The signal was amplified with a low-noise preamplifier (SR 560 with 12 db/octave 10 kHz high-pass filter) and digitized at 8-bit resolution using a Gage digital oscilloscope card attached to a PC.

The basic measurement that we make consists of the vertical component of particle velocity measured at 1 cm increments or *offsets*, along a line extending perpendicularly from the transducer to a maximum offset of 10 cm. We refer to such a measurement as a *constant-angle section*. The line along which the measurement is made defines an angle relative to the orientation of the grooves. We recorded constant-angle sections from 0 to 90 degrees, with 10 degree spacing; 0 degrees being parallel to the grooves. Thus there are a total of 100 traces (10 angles and 10 offsets).

Figure 2 shows a small subset of the data. It consists of one constant-angle section (in this case the angle is 50 degrees) and one *constant-offset section* (traces for all angles at a fixed source/receiver distance). As shown in SVW, 0 degree propagation is essentially identical to propagation on the smooth surface of aluminum,

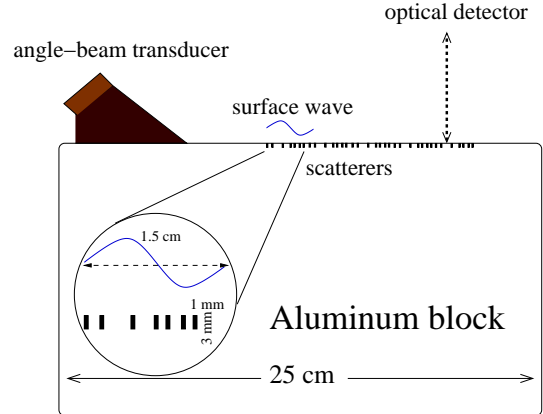


**Figure 1.** The angle-beam transducer launches nearly-plane surface waves of dominant wavelength 15 mm into the grooved block.

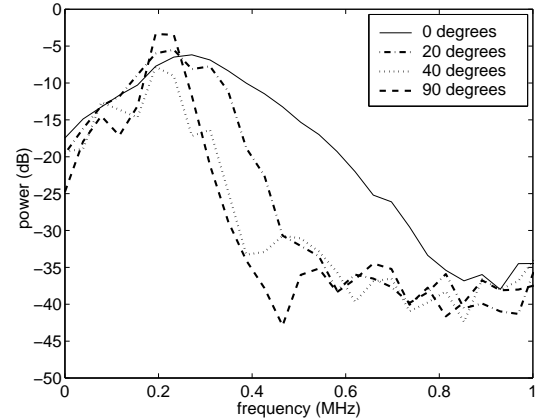


**Figure 3.** Power spectrum of the 5 cm offset data for propagation angles.

which is attenuation- and dispersion-free. However, as the angle of the propagation increases, scattering starts to become significant. In the constant-offset section we can see a clear transition from ballistic propagation to strong multiple-scattering as the angle is increased.

## 3 DATA ANALYSIS

In the absence of scattering, the dominant frequency is around 250 kHz. However, scattering reduces the high frequency power in the data, because the 3mm deep grooves trap the shallower traveling high frequencies more effectively. In Figure 3 we show the power spectrum at 4 different angles computed for a 5 cm constant-offset data.

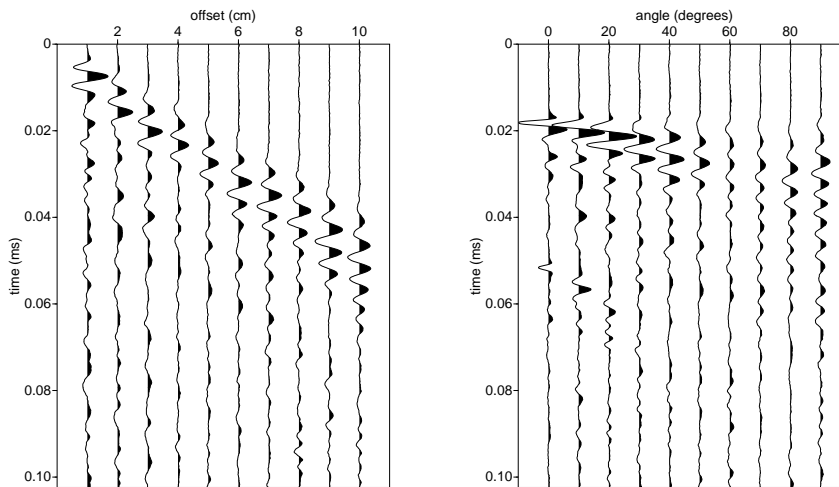


Figure 2. On the left is a constant-angle section (50 degrees). On the right is a constant-offset section (5 cm offset).

### 3.1 Group Velocity

The longer effective path lengths of the multiply-scattered waves results in a significant slowing down of the energy propagation. To estimate the group velocity as a function of angle, we sorted the data into constant-angle sections and then computed the magnitude of the Hilbert transform at each offset. The peaks of these curves were picked automatically and the times taken to be the arrival times of the pulse. This gives an arrival time for each offset, the set of which were fit with a straight line to arrive at the group velocity (Figure 5). The error bars are 98% coverage intervals from the regression. An example of a Hilbert transform contour plot is shown in Figure 4.

Except for angles 60-80 degrees these contours were easy to pick. However, because of the very strong scattering attenuation at these angles (even more so than at 90 degrees) picking peaks of the Hilbert transforms is reliable only for the first 3 or 4 offsets. For these angles we used only the near offset traces to estimate the group velocities. To be conservative however, we kept the error bars from the regression at all offsets, which are larger than would have been the case if they had been estimated from just the near offsets. In any case, it is clear that a linear decrease in group velocity with angle from about 2.9 mm/ $\mu$ s to about 1.9 mm/ $\mu$ s is reasonably consistent with the data.

### 3.2 Mean free path

Even though it is not a truly random medium, we can exploit the spatial disorder of the Fibonacci grooves (Carpena *et al.*, 1995) to estimate the scattering mean free path of the medium as well as to study the trans-

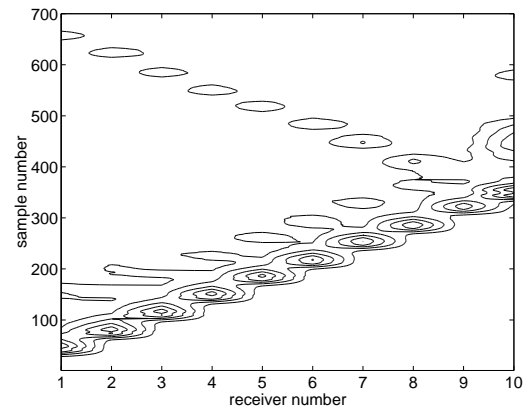
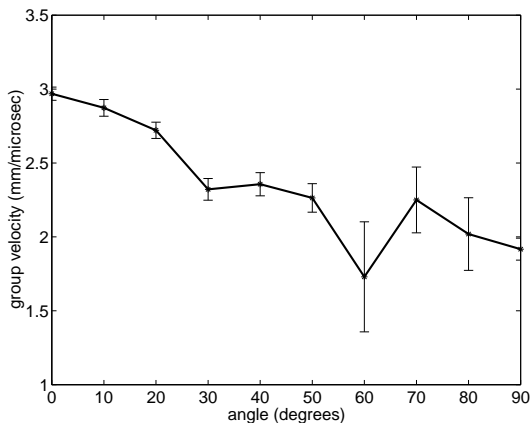


Figure 4. Contour of normalized Hilbert transform (for 0 degree propagation) used for estimating the group velocity. The direct and reflected surface waves are the only events visible.

port of energy. Figure 6 shows traces recorded at a fixed offset of 50 mm, for 38 different positions in the medium. The location of the fixed source/receiver pair was incremented between shots by 1 mm along the source/receiver axis, perpendicular to the grooves. These traces have been corrected for minor positioning errors by aligning the traces. This was done by cross correlating each trace with the average trace and then using the time associated with the peak of this cross-correlation as a static time shift.

Let  $u(\mathbf{r}_i, t)$  denote one of 38 realizations the measured field (particle velocity)  $u$ . Appealing to ergodicity, we will treat the 38 different traces as 38 realizations of a time-varying random process  $u_i(\mathbf{r}, t)$ . We use angle



**Figure 5.** Group velocity as a function of angle.

brackets  $\langle, \rangle$  to denote expectation with respect to this random process. The coherent field is then  $\langle u \rangle$ . The total field can be expressed  $u = \langle u \rangle + u_f$ , where  $u_f$  is the fluctuating part of the field.

All intensities are ensemble averaged intensities. The total intensity  $I_t$  is the intensity of the total field:  $I_t = \langle |u|^2 \rangle$ . The coherent intensity is  $I_c = |\langle u \rangle|^2$ , and the incoherent intensity is  $I_i = \langle |u_f|^2 \rangle$ . By definition

$$I_t = \langle (|u\rangle + |u_f\rangle)^2 \rangle,$$

which will be equal to the sum of the coherent and incoherent intensities plus cross terms which are assumed to average to zero. This is equivalent to assuming that the coherent and incoherent fields are uncorrelated.

Let  $\sigma_t$ ,  $\sigma_a$  and  $\sigma_s$  denote respectively the total, absorption and scattering cross-sections. For a plane wave normally incident in a semi-infinite medium filled with random scatterers, the coherent intensity is expected to decay exponentially as:  $I_c = I_0 \exp(-\rho\sigma_t z)$ , where  $\rho$  is the density of scatterers and  $z$  denotes the distance traveled (see (Ishimaru, 1997), section 14-3). On the other hand the total intensity depends primarily on the absorption and decays as:  $I_t = I_0 \exp(-\rho\sigma_a z)$ . Therefore if we take the ratio of these two intensities, we get a decay that depends only on the scattering cross-section (Rosny & Roux, 2000):

$$\frac{I_c}{I_t} = \frac{I_0 \exp(-\rho\sigma_t z)}{I_0 \exp(-\rho\sigma_a z)} = \frac{\exp(-\rho(\sigma_a z + \sigma_s z))}{\exp(-\rho\sigma_a z)} = \exp(-\rho\sigma_s z).$$

We can express this spatial decay as a temporal decay as follows:

$$\exp(-\rho\sigma_s z) = \exp(-\rho v \sigma_s t) = \exp(-t/\tau_s),$$

where  $v$  is the group velocity and  $\tau_s$  is the scattering mean free time.

To apply this result we compute the coherent and total intensities; numerically,  $I_c$  is just the intensity of the average trace, while  $I_t$  is the average of the intensities of the individual traces. The ratio of  $I_c$  to  $I_t$  is

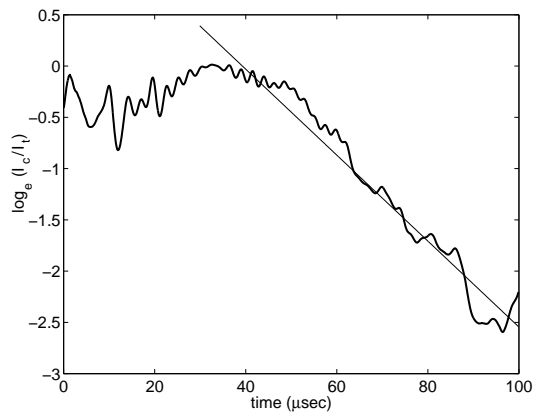


**Figure 7.** Ratio of coherent to total intensities averaged over the ensemble of realizations. The curve decays after the coherent arrival. This decay is fit with an exponential the decay constant of which is the mean free time; in this case,  $24 \mu\text{s}$ .

shown in Figure 7. By fitting an exponential to the portion of the curve after the coherent arrival (about  $30 \mu\text{s}$ ) we get a mean free time  $\tau_s = 24 \mu\text{s}$ . Since this measurement is for propagation at 90 degrees with respect to the grooves, the group velocity is around  $2 \text{ mm}/\mu\text{s}$ , which gives a mean free path of just under 5 cm. Thus we are in a regime in which the wavelength is large compared to the size of an individual scatterer, but small compared to the mean free path; while we have measurements with source-receiver offsets as large as 2 mean free paths. In this sense we can see the complete transition from ballistic to diffusive propagation, even though, strictly speaking, there is no such thing as diffusion in a 1-D random medium, since any random disorder is localizing (Scales & Van Vleck, 1997).

The coherent intensity itself is shown in Figure 8 along with a least-squares fitting model. The model is for a 1-D diffusing medium with attenuation. The attenuation is included to model the effects of small diffractive losses off the bottom of the grooves. The coefficients to be determined from the fitting procedure are the absorption coefficient  $\kappa$  and diffusion constant  $D$  in the Green's function:

$$I(x, t) = (4\pi Dt)^{-1/2} \exp\left(-\frac{x^2}{4Dt} - D\kappa^2 t\right).$$

This result is derived in appendix A.

## 4 CONCLUSIONS

In order to understand the behavior of multiply scattered waves, we have developed an ultrasonic laboratory model of a quasi 1-D medium in which we can not only vary the strength of the scattering, but also measure the wave-field inside the scattering medium in a non-contact manner using a laser-Doppler vibrometer.

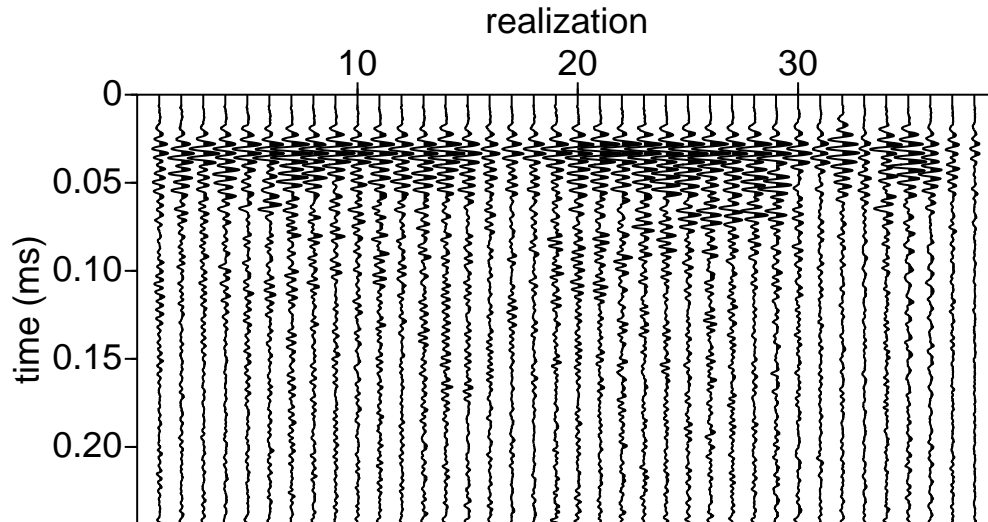


**Figure 6.** 38 traces recorded at a fixed offset of 5 cm on the block. The source/receiver combination was offset by 1 mm between shots.

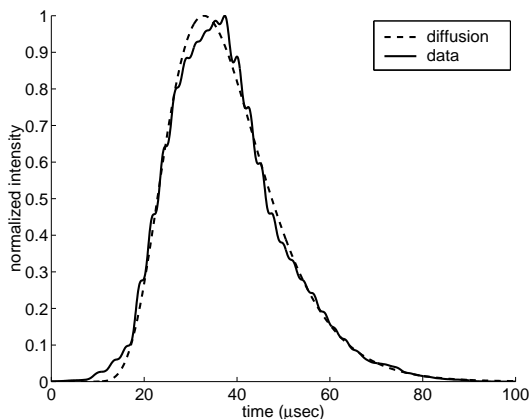


**Figure 8.** Fit of intensity to a model involving propagation in a 1-D diffusive, attenuative medium. The attenuation is used as an approximation to diffractive losses off the bottom of the grooves. The least-squares fit value of the diffusion and attenuation constants are  $D = 3.2 \text{ mm}^2/\mu\text{s}$  and  $\kappa = 0.2 \text{ mm}^{-1}$ , as described in appendix A. The fitted values of the diffusion and attenuation constants are preliminary. Because of the trade-off between these parameters the uncertainties in our estimates could be large. This is the subject of on-going research.

With this system we have observed a clear and reproducible transition from ballistic to diffusive propagation as the strength of the scattering is increased. We have also measured the scattering-dependent group velocity of the medium and shown how the difference between coherent and incoherent averaging of the wave-field can be exploited to give the scattering mean-free path.

## ACKNOWLEDGMENTS

We acknowledge many stimulating discussions with Roel Snieder of CSM and Philippe Roux and Julien De Rosny of the Laboratoire Ondes et Acoustique, École Supérieure de Physique et de Chimie Industrielles de la Ville de Paris. This work was begun while JS was on sabbatical in the ESPCI. He wishes to express his gratitude to his colleagues in Paris for their hospitality. This work was partially supported US Army Research Office under grant #DAAG55-98-1-0070, by the sponsors of the Consortium Project on Seismic Inverse Methods for Complex Structures at the Center for Wave Phenomena, The French Academy of Sciences and the Elf Foundation.

## REFERENCES

- Aki, K., & Chouet, B. 1975. Origin of coda waves: source, attenuation and scattering effects. *Journal of Geophysical Research*, **80**, 3322–3342.
- Backus, G. 1962. Long wavelength anisotropy. *Journal of Geophysical Research*, **67**, 4427–4440.
- Bizheva, K.K., Siegel, A.M., & Boas, D.A. 1998. Path-length-resolved dynamic light scattering in highly scattering random media: The transition to diffusing wave spectroscopy. *Physical Review*, **E58**, 7664–7667.
- Boas, D.A., Campbell, L.E., & Yodh, A.G. 1995. Scattering and imaging with diffusing temporal field correlations. *Physical Review Letters*, **75**, 1855–1858.
- Carpena, P., Gasparian, V., & Ortuno, M. 1995. Energy spectra and level statistics of Fibonacci and Thue-Morse chains. *Physical Review B*, **51**, 12813–12816.
- Derode, A., Roux, P., & Fink, M. 1995. Robust acoustic

- time reversal with high-order multiple scattering. *Physical Review Letters*, **75**, 4206–4209.
- Groenenboom, J., & Snieder, R. 1995. Attenuation, dispersion and anisotropy by multiple scattering of transmitted waves through distributions of scatterers. *J. Acous. Soc. America*, **98**, 3482–3492.
- Ishimaru, A. 1997. *Wave Propagation and Scattering in Random Media*. Oxford University Press.
- O'Doherty, R. F., & Anstey, N. A. 1971. Reflections on amplitudes. *Geophysical Prospecting*, **19**, 430–458.
- Rosny, J. De, & Roux, P. 2000. preprint.
- Scales, J.A., & Snieder, R. 1999. What is a Wave? *Nature*, **401**, 739–740.
- Scales, J.A., & Van Vleck, E.S. 1997. Lyapunov exponents and localization in randomly layered media. *Journal of Computational Physics*, **133**, 27–42.
- Scales, J.A., & Van Wijk, K. 1999. Multiple scattering attenuation and anisotropy of ultrasonic surface waves. *Applied Physics Letters*, **74**, 3899–3901.
- Snieder, R. 1999. Imaging and averging in complex media. In: Fouque, J.-P. (ed), *Diffuse waves in complex media*. Kluwer.
- Wolfe, J. 1998. *Imaging Phonons: acoustic wave propagation in solids*. Cambridge University Press.

## APPENDIX A: GREEN'S FUNCTION

To find the Green's function, we solve the 1-D diffusion equation with attenuation using a delta function source:

$$\frac{\partial I}{\partial t} - D \frac{\partial^2 I}{\partial x^2} + D\kappa^2 I = \delta(x)\delta(t), \quad (\text{A1})$$

where  $D$  is the diffusion constant,  $\delta(x)\delta(t)$  the source term, and  $\kappa$  an absorption coefficient, caused by diffraction from the bottom of the grooves. In the  $(\omega, k)$  domain, it follows that:

$$I(\omega, k) = \frac{1}{D(k^2 + \kappa^2) - i\omega} \quad (\text{A2})$$

so the intensity as a function of space and time is

$$\begin{aligned} I(t, x) &= \frac{1}{(2\pi)^2} \int_{-\infty}^{\infty} \int_{-\infty}^{\infty} \frac{e^{-ikx} e^{-i\omega t} dk d\omega}{D(k^2 + \kappa^2) - i\omega} \\ &= (4\pi Dt)^{-1/2} \exp\left(-\frac{x^2}{4Dt} - D\kappa^2 t\right). \end{aligned} \quad (\text{A3})$$